ISSN 0006-2979, Biochemistry (Moscow), 2008, Vol. 73, No. 2, pp. 200-208. © Pleiades Publishing, Ltd., 2008.
Published in Russian in Biokhimiya, 2008, Vol. 73, No. 2, pp. 247-257.
Originally published in Biochemistry (Moscow) On-Line Papers in Press, as Manuscript BM07-256, November 11, 2007.

Phosphorylation by Cyclic AMP-Dependent Protein Kinase Inhibits Chaperone-Like Activity of Human HSP22 *in vitro*

A. A. Shemetov, A. S. Seit-Nebi, O. V. Bukach, and N. B. Gusev*

Department of Biochemistry, Faculty of Biology, Lomonosov Moscow State University, 119991 Moscow, Russia; fax: (495) 939-2747; E-mail: NBGusev@mail.ru

Received July 23, 2007
Revision received August 8, 2007

Abstract—Human small heat shock protein with molecular mass 22 kD (HSP22, HspB8) contains two Ser residues (Ser24 and Ser57) in consensus sequence RXS and is effectively phosphorylated by cAMP-dependent protein kinase *in vitro*. Mutation S24D did not affect, whereas mutations S57D or S24,57D prevented phosphorylation of HSP22 by cAMP-dependent protein kinase thus indicating that Ser57 is the primary site of phosphorylation. Phosphorylation (or mutation) of Ser57 (or Ser24 and Ser57) resulted in changes of the local environment of tryptophan residues and increased HSP22 susceptibility to chymotrypsinolysis. Mutations mimicking phosphorylation decreased dissociation of HSP22 oligomer at low concentration without affecting its quaternary structure at high protein concentration. Mutations S24D, S57D, and especially S24,57D were accompanied by decrease of chaperone-like activity of HSP22 if insulin and rhodanase were used as substrates. Thus, phosphorylation by cAMP-dependent protein kinase affects the structure and decreases chaperone-like activity of HSP22 *in vitro*.

DOI: 10.1134/S0006297908020120

Key words: small heat shock proteins, phosphorylation, structure, chaperone-like activity

Small heat shock proteins (sHSP) form a large family of ubiquitous proteins expressed in all kingdoms (archae, bacteria, lower and higher eukaryotes) except of some pathogenic bacteria [1, 2]. These proteins differ in their molecular mass that ranges from 12 to 43 kD and possess a conservative α-crystallin domain containing 80-100 amino acid residues and usually located in the C-terminal part of the molecule [1, 2]. The α-crystallin domain is flanked by highly mobile, variable, and different in size N-terminal and C-terminal ends [3]. Small heat shock proteins tend to form high molecular mass oligomers [4, 5] composed of identical or non-identical subunits that under certain conditions can be easily exchanged [6, 7].

The human genome encodes ten different small heat shock proteins (HspB1-HspB10) [8, 9]. These proteins differ in abundance and tissue specificity. Many human small heat shock proteins undergo phosphorylation, and this modification affects their structure and properties. HSP27 (HspB1) is phosphorylated at Ser15, Ser78, and Ser82 by MAPKAP2 kinase [10], and phosphorylation of Ser78 and Ser82 affected formation of oligomeric complexes, whereas phosphorylation of Ser15 might be important for chaperone-like activity [11]. Human αB-crystallin (HspB5) is phosphorylated by MAPKAP2 kinase at Ser59, by p44/42 MAPK at Ser45, and at Ser19 by an unknown kinase [12]. Phosphorylation of Ser19 did not significantly affect the quaternary structure and chaperone-like activity of αB-crystallin, whereas phosphorylation of Ser45 (or mutations mimicking phosphorylation) decreased the size of oligomers or destabilized dimeric substructure of αB-crystallin and affected chaperone-like activity of this protein [13, 14]. Human HSP20 (HspB6) can be phosphorylated by several different protein kinases, and phosphorylation of Ser16 by cyclic-nucleotide-dependent protein kinases modulated HSP20-dependent relaxation of smooth muscle [15], cardioprotective action of HSP20 [16], and its chaperone activity [17]. Recently published data indicate that phosphorylation (or mutations mimicking phosphorylation)

Abbreviations: PMSF) phenylmethanesulfonyl fluoride; sHSP) small heat shock proteins; TLCK) N_α-tosyl-L-lysine chloromethyl ketone hydrochloride; TPCK) N_α-tosyl-L-phenylalanine chloromethyl ketone.

* To whom correspondence should be addressed.

might affect intersubunit interaction between different small heat shock proteins [18].

Initially human HSP22 (HspB8) was described as a protein similar to the protein kinase domain of the large subunit of herpes simplex virus type 2 ribonucleotide reductase and was designed as H11 kinase that was postulated to possess endogenous protein kinase activity [19]. Later it was shown that HSP22 is a typical small heat shock protein possessing a conservative α-crystallin domain [20] and able to interact with many other small heat shock proteins [18]. Some properties of HSP22 were investigated [21, 22], and its endogenous protein kinase activity was questioned [23]. Although intrinsic protein kinase activity of HSP22 remains questionable, the data of the literature [20] indicate that in the cell HSP22 is present in multiple forms that differ in isoelectric points and that probably correspond to differently phosphorylated species. HSP22 can be phosphorylated by protein kinase C and by p44 MAP kinase *in vitro* [20] and is coimmunoprecipitated [24] and weakly phosphorylated by casein kinase 2 [20].

In addition to its well-documented chaperone-like activity [21, 22, 25], HSP22 seems to be involved in regulation of apoptosis [24, 26], myocardial hypertrophy [27], or cell proliferation [28]. It is possible that all these activities can be somehow regulated by HSP22 phosphorylation. However, the effect of phosphorylation on HSP22 properties remained uninvestigated. Therefore, this presentation deals with investigation of *in vitro* phosphorylation of HSP22 by cyclic AMP-dependent protein kinase and the effect of HSP22 phosphorylation on some of its properties.

MATERIALS AND METHODS

Obtaining HSP22 mutants. Point mutations mimicking phosphorylation of S24D, S57D, and S24,57D of HSP22 were generated according to the two-step PCR-based "megaprimer" method [29]. S24D was obtained using S24D 5′-TTCCGGGACGACCCCCTCTCC as forward primer, standard T7-terminator primer as reverse, and pET23-hHSP22 [21] as a template at the first step PCR. The resulting 620-bp PCR product was purified in 1% agarose gel and then used at the second step PCR as reverse "megaprimer" together with standard T7-promoter primer and pET23-hHSP22 plasmid. The final 760-bp PCR product was purified in 1% agarose gel, treated with *Nde*I and *Xho*I restrictases, and ligated into pET23b vector treated with the same restrictases.

The S57D mutation was obtained with the same approach as S24D, using S57D 5′-CTCGTCTCGACTCCGCCTGGC and T7-terminator primer at the first step. At the second step, the resulting 520 bp "megaprimer" was extended using standard T7 terminator primer.

Double mutant S24,57D was generated in the same way as S57D but using pET23-hHSP22-S24D as template in PCR. Pfx DNA polymerase (Invitrogen, USA) was utilized according to manufacturer's instructions. In all cases the presence of mutation and integrity of HSP22 coding sequence was confirmed by DNA sequencing.

Expression and purification of HSP22. Wild type human HSP22 and its pseudophosphorylation mutants were expressed in *E. coli* BL21(DE3) and purified as described earlier [21, 30]. All proteins were concentrated to 4-6 mg/ml and stored frozen in buffer B (20 mM Tris-acetate, pH 7.6, containing 10 mM NaCl, 15 mM mercaptoethanol, 0.1 mM EDTA, and 0.1 mM phenylmethanesulfonyl fluoride (PMSF)).

Protein phosphorylation. The wild type HSP22 and its mutants (0.5-0.7 mg/ml) in buffer P (15 mM potassium phosphate, 15 mM Tris (pH 7.3) containing 5.5 mM $MgCl_2$, 1.5 mM dithiothreitol, and 0.1 mM PMSF) were phosphorylated by the catalytic subunit of cAMP-dependent protein kinase (Sigma, USA) (0.02 unit/μl). The incubation mixture (230-250 μl) contained [γ-^{32}P]ATP (3.5 MBq/ml), and the final concentration of ATP was 200 μM. The samples were incubated at 37°C, and aliquots of 20 μl were spotted on Whatman 3MM filters at different time of incubation, washed in 10% trichloroacetic acid containing 5 mM sodium phosphate and 5 mM sodium pyrophosphate, and after drying counted on a scintillation counter.

Electrophoretic methods. SDS-electrophoresis on gradient (7-20%) or homogeneous 15% polyacrylamide gels was performed according to Laemmli [31]. Native gel electrophoresis was run on 15% polyacrylamide gels in 80 mM Tris-glycine, pH 8.6. In the case of radioactive samples, electrophoresis was followed by autoradiography [32].

Fluorescence spectroscopy. Fluorescence measurements were performed in buffer F (50 mM phosphate (pH 7.5) containing 150 mM NaCl and 2 mM dithiothreitol) on a Hitachi F3000 spectrofluorometer (Hitachi, Japan) at 25°C. The fluorescence of protein samples (0.06 mg/ml) was excited at 295 nm (slit width 5 nm) and recorded in the range 300-400 nm (slit width 1.5 nm). The fluorescence spectra were decomposed into individual components corresponding to Trp residues located in different environment [33].

Limited proteolysis. Trypsinolysis of HSP22 and its pseudophosphorylated mutants was performed in 20 mM Tris-acetate (pH 7.6) containing 10 mM NaCl and 30 mM mercaptoethanol at 37°C at protein concentration 0.6-0.7 mg/ml and at weight ratio HSP22/TPCK-treated trypsin (Sigma) equal to 12,000 : 1. Chymotrypsinolysis was performed under identical conditions except of the ratio HSP22/TLCK-treated chymotrypsin that was equal to 1200 : 1. The reaction was started by addition of protease and after different time of incubation was stopped by addition of PMSF to the final concentra-

tion 0.1 mM. The composition of the samples was analyzed by SDS gel electrophoresis. The apparent rate constant of proteolysis was determined by plotting $\ln(A_t/A_0)$ (where A_0 and A_t correspond to the intensity of the band of intact protein at zero time of incubation and at time t) against time of incubation.

Chemical crosslinking. Chemical crosslinking was performed at fixed concentration of dimethylsuberimidate (3 mM) and at protein concentrations varying from 0.08 to 1.6 mg/ml. Protein samples (20 µl) in buffer B (20 mM Tris-acetate, pH 7.6, 10 mM NaCl, 0.1 mM EDTA, 15 mM mercaptoethanol, 0.1 mM PMSF) were mixed with equal volume of 6 mM dimethylsuberimidate dissolved in 0.4 M triethanolamine-HCl, pH 8.0, containing 30 mM mercaptoethanol. After incubation at 37°C for 1 h, the reaction was stopped by addition of SDS sample buffer, and the protein composition was determined by SDS gel electrophoresis [31].

Size-exclusion chromatography. Oligomeric structure of HSP22 and its pseudophosphorylated mutants was analyzed by size-exclusion chromatography performed on a Superdex 75 HR 10/30 column in buffer S (20 mM Tris-acetate, pH 7.6, containing 150 mM NaCl, 0.1 mM EDTA, 15 mM mercaptoethanol, and 0.1 mM PMSF) using an ACTA FPLC chromatograph (Pharmacia, Sweden). The protein sample (150 µl) containing 10-200 µg of HSP22 or its mutants was loaded in a 500 µl loop and subjected to chromatography at the flow rate 0.5 ml/min. The column was calibrated with the following protein standards: bovine serum albumin (68 kD), ovalbumin (43 kD), chymotrypsinogen (25 kD), and RNase A (13.7 kD).

Chaperone-like activity. Chaperone-like activity of HSP22 was determined by its ability to prevent aggregation of partially denatured protein. In the first case, 130 µl of insulin (0.4 mg/ml) in 100 mM phosphate (pH 7.2) containing 100 mM NaCl was mixed with equal volume of buffer B (20 mM Tris-acetate, pH 7.6, 10 mM NaCl, 0.1 mM EDTA, 15 mM mercaptoethanol, 0.1 mM PMSF) containing variable quantities of HSP22 or its mutants. The sample was incubated at 37°C and reaction was started by addition of dithiothreitol to the final concentration 20 mM. Reduction of insulin disulfide bonds results in dissociation and aggregation of B-chain that was followed by increase in the optical density at 360 nm. In the second case, rhodanase (Fluka, Switzerland) was dissolved in 100 mM phosphate (pH 7.0) containing 100 mM NaCl to the final concentration 0.4 mg/ml. A 120-µl sample of rhodanase was mixed with equal volume of buffer B containing variable quantities of HSP22 and 20 µl of 320 mM solution of dithiothreitol and incubated 10 min at 37°C. Afterwards the samples were transferred to thermostatted cell holder heated to 44°C and heat-induced aggregation of rhodanase was followed by increase of optical density at 360 nm. All optical measurements were performed on an Ultrospec 3100 Pro spectrophotometer.

RESULTS

Phosphorylation of HSP22 by cAMP-dependent protein kinase. Data in the literature [20] indicate that *in vitro* HSP22 is phosphorylated by p44 MAP-kinase, protein kinase C, and to a smaller extent by casein kinase 2. Analyzing the primary structure of human HSP22 by the NetPhos program (http://www.cbs.dtu.dk/services/NetPhos), we detected two sites that could be phosphorylated by cAMP-dependent protein kinase. The primary structure at Ser24 (RDSPL) and at Ser57 (RLSSA) of HSP22 correlates with consensus sequence (RXS) recognized by cAMP-dependent protein kinase in different substrates. Indeed, incubation of HSP22 with the catalytic subunit of cAMP-dependent protein kinase was accompanied by rapid incorporation of radioactive phosphate (Fig. 1a), and after prolonged incubation the extent of phosphorylation was close to 1 mole of phosphate per mole of protein.

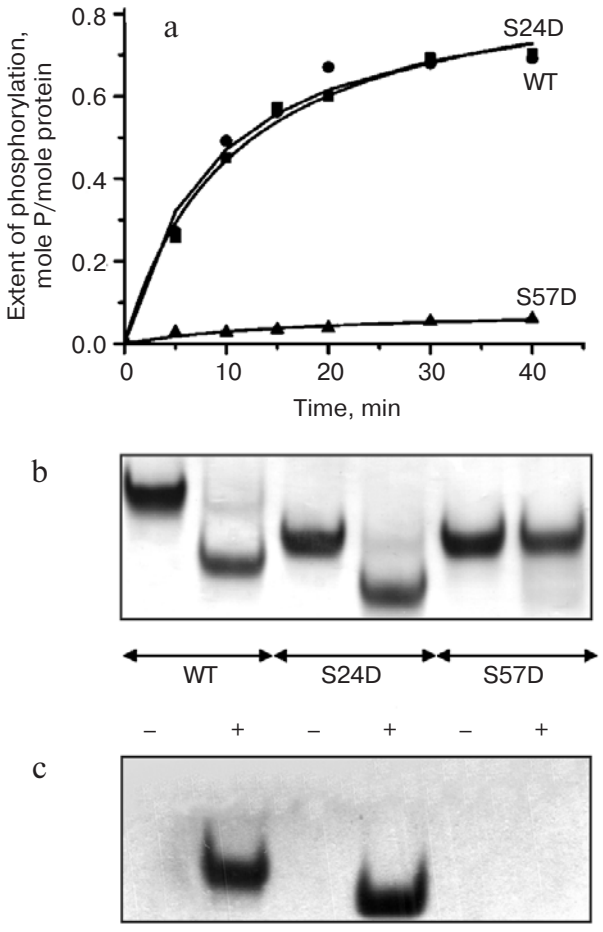

Fig. 1. Phosphorylation of HSP22 by cAMP-dependent protein kinase. a) Kinetics of phosphorylation of wild type (WT) HSP22 and its S24D and S57D mutants. b) Native gel electrophoresis of the wild type HSP22 and its S24D and S57D mutants before (–) and after (+) phosphorylation. c) Autoradiography of the same gel.

To determine the sites phosphorylated by cAMP-dependent protein kinase, we obtained three mutants (S24D, S57D, and S24,57D) mimicking phosphorylation at these sites and phosphorylated the wild type protein and phosphomimicking mutants of HSP22 with cAMP-dependent protein kinase under identical conditions. The rate and extent of S24D mutant phosphorylation was indistinguishable from that of the wild type protein (Fig. 1a). At the same time, both S57D (Fig. 1a) and S24,57D (data not shown) mutants were poor substrates for cAMP-dependent protein kinase.

Phosphorylation of the wild type HSP22 by cAMP-dependent protein kinase is accompanied by increase of its electrophoretic mobility under non-denaturing conditions. After incorporation of 1 mole phosphate per mole of HSP22 the band of unphosphorylated protein completely disappeared and was replaced by a new band having higher electrophoretic mobility (Fig. 1b). Replacement of neutral Ser24 by negatively charged Asp in S24D mutant results in increased electrophoretic mobility compared with unphosphorylated wild type HSP22 (Fig. 1b). Phosphorylation of S24D mutant by cAMP-dependent protein kinase resulting in incorporation of 1 mole phosphate per mole of protein is accompanied by disappearance of the band corresponding to the unphosphorylated protein and appearance of a new radioactive band with higher electrophoretic mobility (Fig. 1, b and c). Incubation of S57D mutant of HSP22 with cAMP-dependent protein kinase resulted in incorporation of only a trace amount of radioactive phosphate (Fig. 1, a and c), and we did not observe any significant change in the electrophoretic mobility of this protein (Fig. 1b). Similar results were obtained with S24,57D mutant (data not shown). The data presented indicate that Ser57 is the primary site phosphorylated by cAMP-dependent protein kinase in HSP22 *in vitro*.

Effect of phosphorylation and mutations mimicking phosphorylation on HSP22 structure. Human HSP22 contains four Trp residues, three of which (Trp48, 51, 60) are located in the N-terminal part of protein molecule close to the potential sites of phosphorylation. Therefore we might suppose that phosphorylation or mutations mimicking phosphorylation will somehow affect intrinsic fluorescence of HSP22. Indeed, phosphorylation by cAMP-dependent protein kinase or mutation S57D induced about 20% increase of intrinsic fluorescence of HSP22, whereas mutations S24D or S24,57D induced even larger (about 30%) increase of Trp fluorescence (Fig. 2a). These changes of fluorescence can be evoked by alterations in Trp environment.

Analysis of spectra of a number of different proteins under different conditions results in formulation of the so-called model of discrete state of Trp residues in the protein molecule [34]. According to this model, there are at least five different discrete states of Trp that differ in hydrophobicity of the environment, accessibility to the solvent and quenchers, and in position of fluorescence maxima [33]. Decomposition of the fluoresce spectrum of the wild type HSP22 reveals three different classes of Trp residues belonging to the so-called classes I, II, and III. Spectral form I corresponds to Trp located inside the protein globule, forming 2 : 1 exciplex with a neighboring polar group and having fluorescence maximum around 330-332 nm. Spectral class II corresponds to Trp residues located on the protein surface in contact with a bound water molecule and having fluorescence maximum at 340-342 nm. Finally, Trp belonging to class III are located on the protein surface, contact with free water molecules, and have fluorescence maximum at 350-353 nm [33]. The fluorescence spectrum of HSP22 can be represented as a sum of three polynomial distributions (of the fourth or fifth order) corresponding to three classes of Trp residues. Varying portion of each class one can estimate

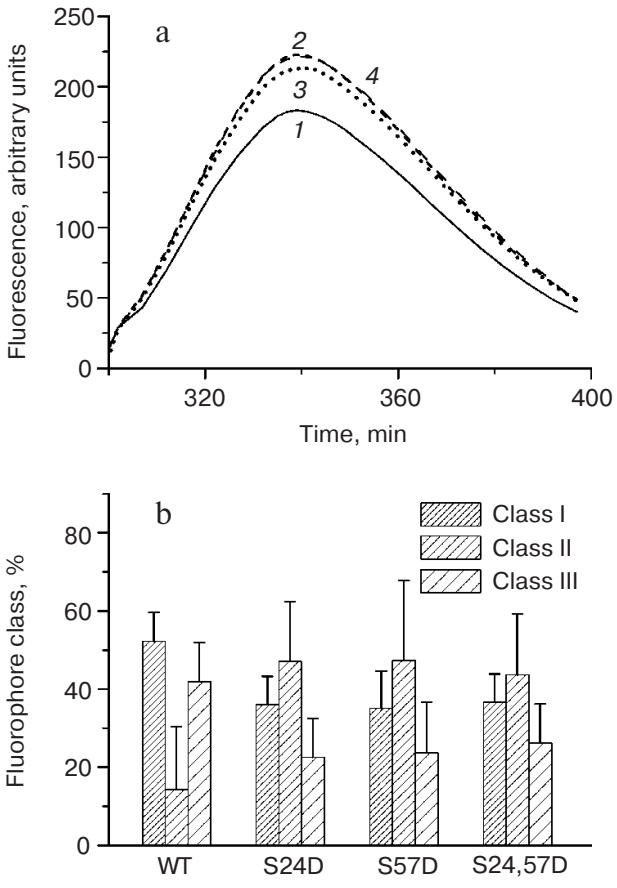

Fig. 2. Intrinsic fluorescence of the wild type HSP22 and its pseudophosphorylated mutants. a) Fluorescence spectra of the wild type HSP22 (*1*) and its S24D (*2*), S57D (*3*), and S24,57D (*4*) mutants. Fluorescence spectra of HSP22 phosphorylated by cAMP-dependent protein kinase (0.9 mole phosphate per mole of protein) were indistinguishable from that of mutant S57D. Protein concentration was 0.06 mg/ml. b) Decomposition of fluorescence spectra of HSP22 and it pseudophosphorylated mutants into components based on the model of discrete states of Trp residues in proteins. Distribution of Trp residues of phosphorylated HSP22 was similar to that of S57D mutant.

contribution of each class of Trp residues in the overall protein fluorescence spectrum. We found that in the wild type protein about 45-50% of the Trp residues belong to class I, about 12-17% to class II, and about 40% to class III Trp fluorophore (Fig. 2b). These data are in good agreement with our earlier results [30] and with the recently published data of Chowdary et al. [35] that were obtained by time-resolved fluorescence measurements. Phosphorylation by cAMP-dependent protein kinase or mutations mimicking phosphorylation lead to redistribution of Trp residues between the three above-mentioned spectral classes. The portion of Trp residues belonging to classes I and III decreased from 45-50 to 35-37% and from 45-50 to 23-26%, respectively, and simultaneously the portion of Trp residues belonging to class II was increased from 12-17 to 43-47% (Fig. 2b). These data indicate that phosphorylation or mutations mimicking phosphorylation affect the structure of the N-terminal part of HSP22.

Limited proteolysis was used for further analysis of the structure of HSP22 and its pseudophosphorylated mutants. HSP22 and its mutants are very susceptible to trypsinolysis, and even at weight ratio HSP22/trypsin equal to 12,000 : 1 we observed rapid cleavage of intact protein and formation of peptides with apparent molecular masses of 23.0, 22.0, 19.0, 18.0, and 16.5 kD (data not shown). These data agree with earlier published results [30]. We did not observe significant difference in the rate of trypsinolysis or in the pattern of tryptic peptides for the wild type protein or its pseudophosphorylated mutants (data not shown). If HSP22 was subjected to chymotrypsinolysis at the weight ratio HSP22/chymotrypsin equal to 1200 : 1, we observed rapid accumulation of peptides with apparent molecular masses of 24.0, 23.5, and 21.8 kD (data not shown). The pattern of chymotryptic peptides was identical for the wild type protein and its pseudophosphorylated mutants, but the rate of chymotrypsinolysis was higher for S57D and S24,57D mutants than for the wild type protein or its S24D mutant. These data correlate with our observation that the double mutant (S24,57D) is very unstable and undergoes proteolytic degradation in the course of purification. The pattern of chymotryptic peptides indicates that the sites of chymotrypsinolysis are located close to the N- or C-terminal ends of HSP22 and that phosphorylation (or mutations mimicking phosphorylation) affects susceptibility of these sites to proteolysis.

Effect of phosphorylation on quaternary structure of HSP22. The majority of the small heat shock proteins tend to form oligomers, and their phosphorylation is often accompanied by dissociation of these oligomers [10, 13]. This makes desirable investigation of phosphorylation (or mutations mimicking phosphorylation) on the quaternary structure of HSP22. Two methods, i.e. chemical crosslinking and size-exclusion chromatography, were used for investigation of the quaternary structure of HSP22.

Crosslinking with dimethylsuberimidate was performed at three protein concentrations (0.08, 0.40, and 1.60 mg/ml). Untreated HSP22 migrated as a band with an apparent molecular mass of 25 kD on the SDS gel electrophoresis. At low protein concentration, crosslinking leads to formation of a new band with apparent molecular mass 50 kD that probably corresponds to crosslinked dimer (data not presented). In addition, the band with apparent molecular mass 25 kD corresponding to monomeric HSP22 became more diffuse, probably due to formation of different intramolecular crosslinks. At low protein concentration (0.08 mg/ml) the intensity of the band of crosslinked dimer for all mutants mimicking phosphorylation was slightly larger than the intensity of the corresponding crosslinked dimer of the wild type protein. After crosslinking at high protein concentration the band with apparent molecular mass 25 kD became very faint, and in addition to the band with apparent molecular mass 50 kD we observed new bands with molecular mass more than 100 kD that probably correspond to crosslinked high molecular mass oligomers of HSP22 (data not shown). At high protein concentrations mutations mimicking phosphorylation do not significantly affect crosslinking of HSP22 with dimethylsuberimidate. These data might indicate that at high concentration the quaternary structure of the wild type HSP22 and its mutants mimicking phosphorylation is similar or identical. At the same time, at low protein concentrations small oligomers of HSP22 start to dissociate, and the wild type protein dissociates more easily than the mutants mimicking phosphorylation. Therefore, at low protein concentration crosslinking of the wild type protein is less probable than crosslinking of its mutants mimicking phosphorylation.

Size-exclusion chromatography was used to check this suggestion. Loading on the column of 70-120 μg of the wild type HSP22, we detected a single peak with apparent molecular mass 33-34 kD (Fig. 3a). In good agreement with the earlier published results [21], we found that in the narrow range of concentrations the elution volume of this peak was only weakly dependent on the quantity on protein loaded on the column. If the same quantities of phosphorylated (or mutated) HSP22 were loaded on the column we also observed a single peak that was eluted slightly earlier than the corresponding peak of the wild type protein and the apparent molecular mass of proteins eluted in this peak was in the range 36-37 kD (Fig. 3a). Although the difference in elution volume was minimal, it was reproduced in three independent experiments. Decrease of the protein load from 100 to 10 μg was accompanied by increase of elution volume of HSP22, and this increase was larger for the wild type protein than for S57D mutant (Fig. 3b). Increase of elution volume might reflect dissociation of HSP22 oligomers. Indeed, decrease of the protein load from 100 to 10 μg resulted in decrease of the apparent molecular mass of the wild type

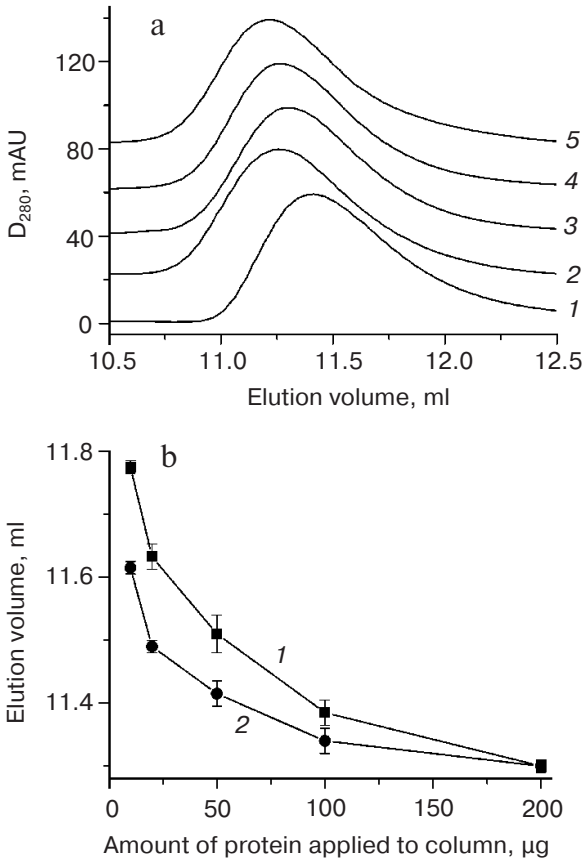

Fig. 3. Analysis of the quaternary structure of HSP22 by size-exclusion chromatography. a) Elution profiles of the wild type HSP22 (*1*), phosphorylated HSP22 (*2*), or S24D (*3*), S57D (*4*), or S24,57D (*5*) mutants. Equal volumes (130 μl) containing 90 μg proteins were loaded on Superdex 75 HR 10/30 column. For clarity, elution profiles are shifted from each other by 20 mAU. b) Dependence of elution volume on the quantity of the wild type HSP22 (*1*) or its S57D (*2*) mutant loaded on the column.

protein from 33-34 to 25-27 kD. Under identical conditions the apparent molecular mass of the S57D mutant was decreased from 36-37 to 30-32 kD, and similar results were obtained with S25,57D. These data might indicate that at high concentration HSP22 and its mutants form similar low molecular mass oligomers (probable dimers) that dissociate upon dilution. Mutations mimicking phosphorylation decrease the probability of dissociation and therefore at low protein concentration the size of oligomers formed by the wild type HSP22 is smaller than the size of corresponding oligomers formed by its pseudophosphorylated mutants.

Chaperone-like activity of HSP22. Chaperone-like activity of HSP22 was determined by its ability to prevent aggregation of partially denatured insulin and rhodanase. Reduction of disulfide bonds of insulin results in dissociation of insulin chains and aggregation of chain B, which is accompanied by increase of light scattering (Fig. 4, curve *1*). Addition of the wild type HSP22 results in retardation of insulin aggregation and decrease of the amplitude of light scattering (Fig. 4, curve *2*). This effect was concentration dependent and was especially large if the weight concentration of HSP22 was equal to that of insulin (Fig. 4c, curve *2*). Phosphorylation by cAMP-dependent protein kinase or mutations mimicking phosphorylation decreased the chaperone-like activity of HSP22, and at equal concentrations phosphorylated (or pseudophosphorylated) HSP22 was less effective than unphosphorylated wild type protein (Fig. 4, a-c). The double mutant S24,57D was especially ineffective in preventing insulin aggregation (Fig. 4c, curve *6*). This mutant retarded the onset of aggregation, but on the later stages of incubation the rate and the maximal amplitude

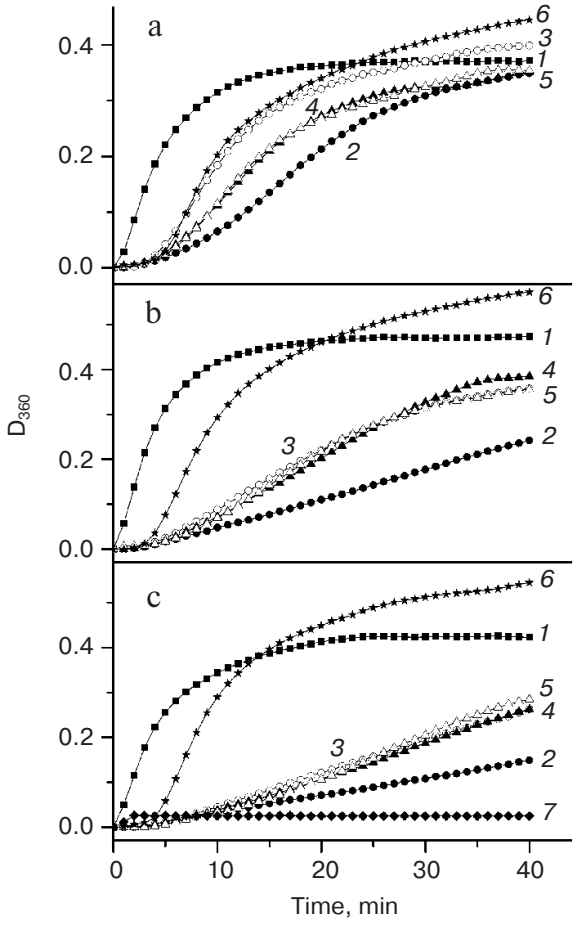

Fig. 4. Chaperone-like activity of HSP22 with insulin as a model substrate. Aggregation of insulin (0.2 mg/ml) was induced by reduction of disulfide bonds and was followed by increase of the optical density at 360 nm in the absence of HSP22 (curve *1*) or in the presence of the wild type HSP22 (curve *2*), phosphorylated by cAMP-dependent protein kinase HSP22 (curve *3*), or S24D (curve *4*), S57D (curve *5*), or S24,57D (curve *6*) mutants of HSP22. Experiments were performed at the final concentration of HSP22 equal to 0.10 (a), 0.15 (b), or 0.20 (c) mg/ml. Curve *7* represents the lack of changes in the optical density of the sample containing 0.20 mg/ml of any HSP22 sample in the absence of insulin.

of aggregation became larger than in the control without addition of chaperone. This might indicate that instead of preventing this mutant provokes aggregation of partially denatured insulin B chain or aggregation of the complex formed between insulin B chain and chaperone.

Rhodanase was used as a second substrate for analyzing chaperone-like activity of HSP22. In this case, heating to 43°C induced denaturation and aggregation of rhodanase, and this process was accompanied by increase in light scattering. Addition of increasing quantities of the wild type HSP22 was accompanied by decrease of the rate and amplitude of rhodanase aggregation (data not shown). S24D and S57D mutants of HSP22 were less effective than the wild type protein in inhibition of rhodanase aggregation, and the double mutant S24,57D demonstrated only very weak chaperone effect (data not presented). These data indicate that phosphorylation or mutations mimicking phosphorylation of certain sites located in the N-terminal domain decreases the chaperone activity of HSP22.

DISCUSSION

Many members of the superfamily of human small heat shock proteins undergo phosphorylation catalyzed by a number of different protein kinases. The sites of sHSP phosphorylation are usually located in the N-terminal part of their structure. Indeed, Ser19 of αB-crystallin [12], Ser16 of HSP20 [15], Ser15 of HSP27 [10], and Ser14 and Ser27 of HSP22 [20] are located in the very N-terminal end of the corresponding small heat shock proteins. Ser45 of αB-crystallin [12], Ser57 (this paper), and Thr63 of HSP22 [20] are located in the central part of the N-terminal domain of the corresponding small heat shock proteins. And finally, Ser59 of αB-crystallin [12], Ser78 and Ser82 of HSP27 [10], as well as Thr87 of HSP22 [20] are located at the end of the N-terminal domain close to the beginning of the α-crystallin domain.

Phosphorylation of the sites located close to α-crystallin domain affects intersubunit interaction of the small heat shock proteins. Phosphorylation (or mutation) of Ser45 (and probably Ser59) destabilizes intersubunit contacts and results either in dissociation [13] or in reorganization of the αB-crystallin oligomers [14]. Phosphorylation (or mutations) of Ser78 and Ser82 of human HSP27 or homologous Ser90 of Chinese hamster HSP27 also leads to destabilization and dissociation of large oligomers of these proteins [36, 37].

Phosphorylation of the sites located at the very N-terminal end of small heat shock proteins usually does not affect their quaternary structure. For instance, phosphorylation (or mutation) of Ser19 has only marginal effect on the quaternary structure of αB-crystallin [14]. Phosphorylation of Ser15 has practically no effect on the oligomeric structure of human or Chinese hamster HSP27 [36, 37]. Finally, phosphorylation (or mutation) of Ser16 has no effect on the quaternary structure of human HSP20 [17].

The functional role of the sites of small heat shock proteins located in the middle of the N-terminal domain remains unknown. In this respect, human HSP22 seems to be especially interesting. The data of Benndorf et al. [20] indicate that *in vitro* HSP22 can be phosphorylated at Thr63 and Thr87 by protein kinase C and p44 mitogen-activated protein kinase, respectively. Our results presented in this paper indicate that HSP22 can be phosphorylated *in vitro* by cAMP-dependent proteins kinase at Ser57. All these sites (Ser57, Thr63) are located in the middle of the N-terminal domain of HSP22, and therefore it was reasonable to analyze effect of phosphorylation (or mutations mimicking phosphorylation) on some properties of HSP22.

We found that phosphorylation of Ser57 was accompanied by increase of intrinsic Trp fluorescence and by the change in distribution of Trp residues between three classes that differ in their accessibility to the solvent (Fig. 2). Similar changes in Trp fluorescence were observed for αB-crystallin with mutation in the N-terminal domain [13]. These changes can be explained by the fact that three out of four Trp residues of HSP22 and two Trp residues of αB-crystallin are located in the N-terminal domain of these proteins, often very close to phosphorylated (or mutated) Ser residues. In any case, the data presented indicate that phosphorylation somehow affects the structure of the N-terminal domain of HSP22.

The effect of phosphorylation on HSP22 structure was confirmed in experiments with limited chymotrypsinolysis. Mobile N-terminal and C-terminal ends of the small heat shock proteins contain the primary sites of trypsinolysis and chymotrypsinolysis [38, 39]. In the case of αB-crystallin trypsin preferentially cleaves peptide bonds locate in the C-terminal part, whereas chymotrypsin predominantly cleaves peptide bonds located in the N-terminal part of the protein [38]. We found that mutations mimicking phosphorylation of Ser24 and Ser57 of HSP22 had no effect on limited trypsinolysis, but increased the apparent rate of chymotrypsinolysis. The double mutant S24,57D was especially unstable and undergoes rapid degradation even in the process of purification. Although we have not determined exact sites of chymotrypsinolysis, we might suppose that the primary sites of chymotrypsinolysis are located in the N-terminal part of HSP22 and phosphorylation (or mutation) of certain sites located in this domain affect susceptibility to proteolysis.

Chemical crosslinking and size-exclusion chromatography were used to analyze effect of phosphorylation of the quaternary structure of HSP22. Mutations mimicking phosphorylation of Ser24 and Ser57 do not significantly affect crosslinking by dimethylsuberimidate

at high protein concentration. Independent of site mutations, we observed formation of dimer of HSP22 with apparent molecular mass 50 kD as well as small quantities of crosslinked oligomer with high molecular mass. At the same time, at low protein concentration the wild type HSP22 was less effectively crosslinked than its mutants mimicking phosphorylation. Therefore, we supposed that the wild type HSP22 is more easily dissociated to monomers than its mutants mimicking phosphorylation. On the size-exclusion chromatography, the elution volumes of phosphorylated or mutated HSP22 were slightly smaller than the elution volume of the wild type protein (Fig. 3a). This difference was very small at high protein concentrations and became much larger at low protein concentration (Fig. 3b). Therefore, we suppose that at high protein concentration both the wild type HSP22 and its mutants are present in the form of low molecular mass oligomers (probably dimer). Dilution results in dissociation of HSP22, and this dissociation is more probable for the wild type protein than for its mutants mimicking phosphorylation. Thus, at low protein concentration phosphorylation (or mutations mimicking phosphorylation) can stabilize the oligomeric structure of HSP22.

All data presented indicate that phosphorylation (or mutations mimicking phosphorylation) affects tertiary and quaternary structure of HSP22, but these changes are not very large. In this respect, the question arises whether phosphorylation (or mutation) affects chaperone-like activity of HSP22. The chaperone-like activity was estimated by the ability of HSP22 to prevent reduction-induced aggregation of insulin and thermal-induced aggregation of rhodanase (Fig. 4). We found that phosphorylation (or mutation) of Ser57 (or Ser24) leads to decrease of chaperone-like activity of HSP22. The double mutant S24,57D possessed especially low chaperone-like activity (Fig. 4). The data of the literature indicate that the small heat shock proteins contain several sites involved in the interaction with partially unfolded proteins. In the case of αB-crystallin, two of these sites are located between residues 9-20 and 43-58 [40], and the N-terminal part of αB-crystallin is shielded from proteolysis by addition of substrate proteins [38]. Although the sites of interaction of HSP22 with substrate proteins are unknown, we might suppose that the N-terminal end is also somehow involved in the binding of client proteins, and therefore phosphorylation of the sites located in this domain might affect the chaperone-like activity of HSP22.

According to predictions of the NetPhos program [41], located in the N-terminal Ser24, Ser27, Ser47, Ser57, Thr63, and Thr87 of HSP22 can be phosphorylated with the highest probability. The same program [42] predicts that Ser24 can be phosphorylated by glycogen synthase kinase 3 and cyclin-dependent protein kinase 5 (cdk5), Ser57 is phosphorylated by cAMP-dependent protein kinase, and Thr87 by p38 MAP-kinase, cdk5, and glycogen synthase kinase 3. These predictions to some extent agree with experimental results obtained *in vitro*. Indeed, the data of Benndorf et al. [20] indicate that Ser27 and Thr87 are phosphorylated by p44 MAP-kinase and Thr63 is phosphorylated by protein kinase C. The data of this paper indicate that Ser57 is phosphorylated by cAMP-dependent protein kinase. Summing up, we conclude that HSP22 contains several potential sites of phosphorylation (Thr63 [20] and Ser57 (this investigation)) located in the central part of its N-terminal domain. It is still unknown whether these sites are phosphorylated *in vivo*. However, the data presented indicate that phosphorylation (or mutations mimicking phosphorylation) of these sites might affect the tertiary and quaternary structure of HSP22 and probably by this means influence its chaperone-like activity that might be important for realization of multiple functions ascribed to HSP22 in the literature.

This investigation was supported by the Russian Foundation for Basic Research (grant No. 07-04-00115).

REFERENCES

1. Haslbeck, M., Franzmann, T., and Buchner, J. (2005) *Nature Struct. Mol. Biol.*, **12**, 842-846.
2. Franck, E., Madsen, O., van Rheede, T., Ricard, G., Huynen, M. A., and de Jong, W. W. (2004) *J. Mol. Evol.*, **59**, 792-805.
3. White, H. E., Orlova, E. V., Chen, S., Wang, L., Ignatiou, A., Gowen, B., Stromer, T., Franzmann, T. M., Haslbeck, M., Buchner, J., and Saibil, H. R. (2006) *Structure*, **14**, 1197-1204.
4. Kim, K. K., Kim, R., and Kim, S. H. (1998) *Nature*, **394**, 595-599.
5. Van Monfort, R. L., Basha, E., Friedrich, K. L., Slingsby, C., and Vierling, E. (2001) *Nat. Struct. Biol.*, **8**, 1025-1030.
6. Sobott, F., Benesch, J. L., Vierling, E., and Robinson, C. V. (2002) *J. Biol. Chem.*, **277**, 38921-38929.
7. Sugiyama, Y., Suzuki, A., Kishikawa, M., Akutsu, R., Hirose, T., Way, M. M. Y., Tsui, S. K. W., Yoshida, S., and Ohno, S. J. (2000) *Biol. Chem.*, **275**, 1095-1104.
8. Kappe, G., Franck, E., Verschuure, P., Boelens, W. C., Leunissen, J. A. M., and de Jong, W. W. (2003) *Cell Stress Chaperones*, **8**, 53-61.
9. Fontaine, J.-M., Rest, J. S., Welsh, M. J., and Benndorf, R. (2003) *Cell Stress Chaperones*, **8**, 62-69.
10. Landry, J., Lambert, H., Zhou, M., Lavoie, J. N., Hickey, E., Weber, L. A., and Anderson, C. W. (1992) *J. Biol. Chem.*, **267**, 794-803.
11. Theriault, J. R., Lambert, H., Chavez-Zobel, A. T., Charest, G., Lavigne, P., and Landry, J. (2004) *Biol. Chem.*, **279**, 23463-23471.
12. Kato, K., Ito, H., Kamei, K., Inaguma, Y., Iwamoto, I., and Saga, S. (1998) *J. Biol. Chem.*, **273**, 28346-28354.
13. Ito, H., Kamei, K., Iwamoto, I., Inaguma, Y., Nohara, D., and Kato, K. (2001) *J. Biol. Chem.*, **276**, 5346-5352.
14. Aquilina, J. A., Benesch, J. L. P., Ding, L. L., Yaron, O., Horwitz, J., and Robinson, C. V. (2004) *J. Biol. Chem.*, **279**, 28675-28680.

15. Beall, A., Bagwell, D., Woodrum, D., Stoming, T. A., Kato, K., Suzuki, A., Rasmussen, H., and Brophy, C. M. (1999) *J. Biol. Chem.*, **274**, 11344-11351.
16. Fan, G.-C., Chu, G., and Kranias, E. G. (2005) *Trends Cardiovasc. Med.*, **15**, 138-141.
17. Bukach, O. V., Seit-Nebi, A. S., Marston, S. B., and Gusev, N. B. (2003) *Eur. J. Biochem.*, **271**, 291-302.
18. Sun, X., Welsh, M. J., and Benndorf, R. (2006) *Cell Stress Chaperone*, **11**, 61-70.
19. Smith, C. C., Yu, Y. X., Kulka, M., and Aurelian, L. (2000) *J. Biol. Chem.*, **275**, 25690-25699.
20. Benndorf, R., Sun, X., Gilmont, R. R., Biederman, K. J., Molloy, M. P., Goodmurphy, C. W., Cheng, H., Andrews, P. C., and Welsh, M. J. (2001) *J. Biol. Chem.*, **276**, 26753-26761.
21. Kim, M. V., Seit-Nebi, A. S., Marston, S. B., and Gusev, N. B. (2004) *Biochem. Biophys. Res. Commun.*, **315**, 796-801.
22. Chowdary, T. K., Raman, B., Ramakrishna, T., and Rao, C. M. (2004) *Biochem. J.*, **381**, 379-387.
23. Kim, M. V., Seit-Nebi, A. S., and Gusev, N. B. (2004) *Biochem. Biophys. Res. Commun.*, **325**, 649-652.
24. Hase, M., Depre, C., Vatner, S. F., and Sadoshima, J. (2005) *Biochem. J.*, **388**, 475-483.
25. Carra, S., Sivilotti, M., Chavez Zobel, A. T., Lambert, H., and Landry, J. (2005) *Human Mol. Gen.*, **14**, 1659-1669.
26. Gober, M. D., Wales, S. Q., and Aurelian, L. (2005) *Front. Biosci.*, **10**, 2788-2803.
27. Depre, C., Hase, M., Gaussin, V., Zajac, A., Wang, L., Hittinger, L., Ghaleh, B., Yu, X., Kudej, R. K., Wagner, T., Sadoshima, J., and Vatner, S. F. (2002) *Circ. Res.*, **91**, 1007-1014.
28. Charpentier, A. H., Bednarek, A. K., Daniel, R. L., Hawkins, K. J., Laflin, S., Gaddis, S., MacLeod, M. C., and Aldaz, C. M. (2000) *Cancer Res.*, **20**, 5977-983.
29. Sarkar, G., and Sommer, S. S. (1990) *Biotechnique*, **8**, 404-407.
30. Kim, M. V., Kasakov, A. S., Seit-Nebi, A. S., Marston, S. B., and Gusev, N. B. (2006) *Arch. Biochem. Biophys.*, **454**, 32-41.
31. Laemmli, U. K. (1970) *Nature*, **227**, 680-685.
32. Vorotnikov, A. V., Shirinsky, V. P., and Gusev, N. B. (1988) *FEBS Lett.*, **236**, 321-324.
33. Permyakov, E. A. (1993) in *Luminescent Spectroscopy of Proteins*, CRC Press, Boca Raton-Ann Arbor-London-Tokyo.
34. Burstein, E. A., Vedenkina, N. S., and Ivkova, M. N. (1973) *Photochem. Photobiol.*, **18**, 263-279.
35. Chowdary, T. K., Raman, B., Ramakrishna, T., and Rao, C. M. (2007) *Biochem. J.*, **401**, 437-445.
36. Lambert, H., Charett, S. J., Bernier, A. F., Guimond, A., and Landry, J. (1999) *J. Biol. Chem.*, **274**, 9378-9385.
37. Rogalla, T., Ehrnsperger, M., Preville, X., Kotlyarov, A., Lutsch, G., Ducasse, C., Paul, C., Wieske, M., Arrigo, A.-P., Buchner, J., and Gaestel, M. (1999) *J. Biol. Chem.*, **274**, 18947-18956.
38. Aquilina, J. A., and Watt, S. J. (2007) *Biochem. Biophys. Res. Commun.*, **353**, 1115-1120.
39. Muchowski, P. J., Hays, L. G., Yates, J. R., and Clark, J. I. (1999) *J. Biol. Chem.*, **274**, 30190-30195.
40. Ghosh, J. G., Estrada, M. R., and Clark, J. I. (2005) *Biochemistry*, **44**, 14854-14869.
41. Blom, N., Gammeltoft, S., and Brunak, S. (1999) *J. Mol. Biol.*, **294**, 1351-1362.
42. Blom, N., Sicheritz-Ponten, T., Gupta, R., Gammeltoft, S., and Brunak, S. (2004) *Proteomics*, **4**, 1633-1649.